

Corrosion of Monel-400 in Aerated Stagnant Arabian Gulf Seawater after Different Exposure Intervals

El-Sayed M. Sherif^{1,4,*}, A. A. Almajid^{1,2}, A. K. Bairamov³, Eissa Al-Zahrani³

¹ Center of Excellence for Research in Engineering Materials (CEREM), College of Engineering, King Saud University, P. O. Box 800, Al-Riyadh 11421, Saudi Arabia

² Department of Mechanical Engineering, College of Engineering, King Saud University, P.O. Box 800, Al-Riyadh 11421, Saudi Arabia

³ Materials and Corrosion Section, Saudi Basic Industries Corporation (SABIC), SABIC Technology Center, P.O. Box 11669, Jubail 31961, Saudi Arabia

⁴ Electrochemistry and Corrosion Laboratory, Department of Physical Chemistry, National Research Centre (NRC), Dokki, 12622 Cairo, Egypt

*E-mail: esherif@ksu.edu.sa

Received: 14 September 2011 / Accepted: 15 October 2011 / Published: 1 November 2011

The corrosion of Monel-400 after varied exposure periods in naturally aerated Arabian Gulf seawater (AGS) has been carried out using gravimetric, cyclic potentiodynamic polarization, chronoamperometry, open-circuit potential, and impedance spectroscopy measurements along with SEM/EDX investigations. Gravimetric data within 160 days showed that the weight loss increased, while the corrosion rate decreased with time. SEM/EDX investigations after 160 days immersion indicated that dissolution of Monel takes place due to the selective dissolution of Ni. The electrochemical measurements confirmed the gravimetric data and proved that severity of uniform corrosion of Monel decreases, while pitting one increases with increasing the exposure period.

Keywords: corrosion; Monel-400 alloy; EIS; polarization; SEM; weight loss

1. INTRODUCTION

Monel-400 is one of the most important nickel based alloys that contains about 60-70 percent nickel, 20-29 percent copper and small amounts of iron, manganese, silicon and carbon. It is a solid solution alloy that can only be hardened by cold working. This alloy was discovered due to the efforts of Robert Crooks Stanley, who worked for the International Nickel Company (INCO) in 1901. It was installed as a sheet roofing membrane in 1908. In the late 1920s, Monel-400 was begun to be used for grocery coolers, countertops, sinks, laundry and food preparation appliances, roofing and flashing.

Monel-400 is characterized by its good corrosion resistance, good weldability and high strength. Therefore, it has been used extensively in many applications such as chemical processing equipment, gasoline and fresh water tanks, crude petroleum stills, valves and pumps, propeller shafts, marine fixtures and fasteners, electrical and electronic components, de-aerating heaters, process vessels and piping, boiler feed water heaters and other heat exchangers, and etc [1-4]. For that when a piece of equipment needs to stand up to interior or exterior corrosive, Monel-400 is the fail-safe solution. It also has higher maximum working temperatures than nickel (up to 540 °C, and its melting point is 1300–1350 °C), which makes it the preferred metal for boiler feed water heaters and other heat exchangers.

Although Monel-400 is known for its ability to stand up to tough corrosive elements, pitting corrosion of Monel-400 occurs when it is exposed to stagnant salt water such as seawater [5]. The corrosion rate of this alloy decreases sharply with increasing nickel content in the alloy. A series of Cu-Ni alloys have been studied in natural sea water and in chloride solutions under different conditions [6–12]. Some of these studies have [7] reported that selective electrodisolution of nickel is predominant; while others [11] have found that the dissolution of copper depends on the composition of the alloy under investigation.

The objective of the present work was to study the anodic dissolution of Monel-400 in the aerated stagnant solutions of Arabian Gulf seawater after varied exposure periods. The experimental work has been carried out using weight-loss measurements after varied immersion periods of 5-160 days. The study was also complemented by a variety of electrochemical techniques along with surface morphology and elemental analysis investigations. Since, pitting corrosion is one of the most destructive forms of localized corrosion and the ability of corrosive ions that present in sea water on the breakdown of a passive film might form on the surface of Monel-400, a particular attention was paid to the effect of stagnant AGS solutions on the pitting corrosion of the alloy.

2. EXPERIMENTAL PROCEDURE

The natural sea water (AGS) was obtained directly from the Arabian Gulf at the eastern region (Jubail, Dammam, Saudi Arabia), and was used as received. An electrochemical cell with a three-electrode configuration was used for electrochemical measurements. Monel-400 rod and sheet (were purchased from Magellan Metals, USA, with the following chemical composition, Ni–63.0% min, Cu–“28-34%” max, Fe–2.5% max, Mn–2.0%, Si–0.5% max, C–0.3% max, and S–0.024%) were used in this study. The Monel rod was used as a working electrode. A platinum foil and a Metrohm Ag/AgCl electrode (in 3 M KCl) were used as counter and reference electrodes, respectively.

The weight loss experiments were carried out using rectangular Monel-400 coupons cut from the Monel sheet. The coupons had dimensions of 4.0 cm length, 2.0 cm width, and 0.4 cm thickness and the exposed total area of 54.02 cm². were grinded successively with metallographic emery paper of increasing fineness of up to 800 grits, and then polished with 1, 0.5 and 0.3µm alumina slurries (Buehler). The electrodes were then washed with doubly distilled water, degreased with acetone, washed using doubly distilled water again and finally dried with pure air. The coupons were weighed

and then suspended in 300 cm³ solutions of Arabian Gulf seawater for different exposure periods between 5 and 160 days. The losses in weight per area (ΔW , g.cm⁻²) and the corrosion rates (K_{Corr} , millimeters/year (mmpy)) over the exposure time were calculated as has been reported before [13, 14].

The SEM investigation and EDX analysis were obtained on the surface of a Monel-400 coupon after its immersion in AGS solution for 160 days. The SEM images were obtained by using a JEOL model JSM-6610LV (Japanese made) scanning electron microscope with an energy dispersive X-ray analyzer attached.

The Monel-400 rods for electrochemical measurements were grinded and polished as for the Monel coupons. The diameter of the working electrode was 1.2 cm with a total exposed area of 1.13 cm². Electrochemical experiments were performed by using an Autolab potentiostat (PGSTAT20 computer controlled) operated by the general purpose electrochemical software (GPES) version 4.9. The cyclic potentiodynamic polarization (CPP) curves were recorded by scanning the potential in the forward direction from -800 to +800 mV then backward from +800 to -800 mV against Ag/AgCl again at the same scan rate, 3.0 mV/s. Chronoamperometric (CA) experiments were carried out by stepping the potential of the Monel-400 electrode at +100 mV versus Ag/AgCl for 120 min. For the PPC and CA experiments, the curves were recorded after the electrode immersion in AGS for 0, 24, and 72 h before measurements. Electrochemical impedance spectroscopy (EIS) tests were performed after 1, 24, and 72 h of the electrode immersion at corrosion potentials (E_{Corr}) over a frequency range of 100 kHz – 10 mHz, with an ac wave of ± 5 mV peak-to-peak overlaid on a dc bias potential, and the impedance data were collected using Powersine software at a rate of 10 points per decade change in frequency.

3. RESULTS AND DISCUSSION

3.1. Weight-loss data and SEM / EDX investigations

The variations of (a) the weight loss (ΔW) and (b) the corrosion rate (K_{Corr}) vs. time for Monel-400 coupons in 300 cm³ of AGS are shown in Fig. 1. The values of ΔW and K_{Corr} were calculated as reported in the previous work [13, 14]. It is clearly recognized that the values of ΔW increased from 5×10^{-5} g/cm² after 5 days to 55×10^{-5} g/cm² after 160 days immersion in the AGS solution at the same condition. This is due to the contentious dissolution of Monel-400 surface under the influence of the high salinity of the Arabian Gulf (47000 ppm). On the other side, the values of K_{Corr} decreased with increasing time, which indicates the development then the accumulation of corrosion products and/or oxides on the Monel surface. These formed components partially protect the surface by reducing its dissolution and so decreasing aggressiveness of AGS by limiting the contact of the active Monel surface to AGS test solution. This agrees with the previous studies [15, 16] and proves the poor performance of Monel-400 in freely aerated stagnant AGS.

Figure 2 shows SEM/EDX investigations for Monel-400 surface after its immersion in AGS solutions for 160 days where, (a) the SEM micrograph for a large area of the surface and (b) the corresponding EDX profile analysis for the selected area on the SEM image, respectively. It is obvious

from Fig. 2a that the surface has a flat area covered with corrosion products in addition to numerous pits, which have almost similar round shapes and different diameters.

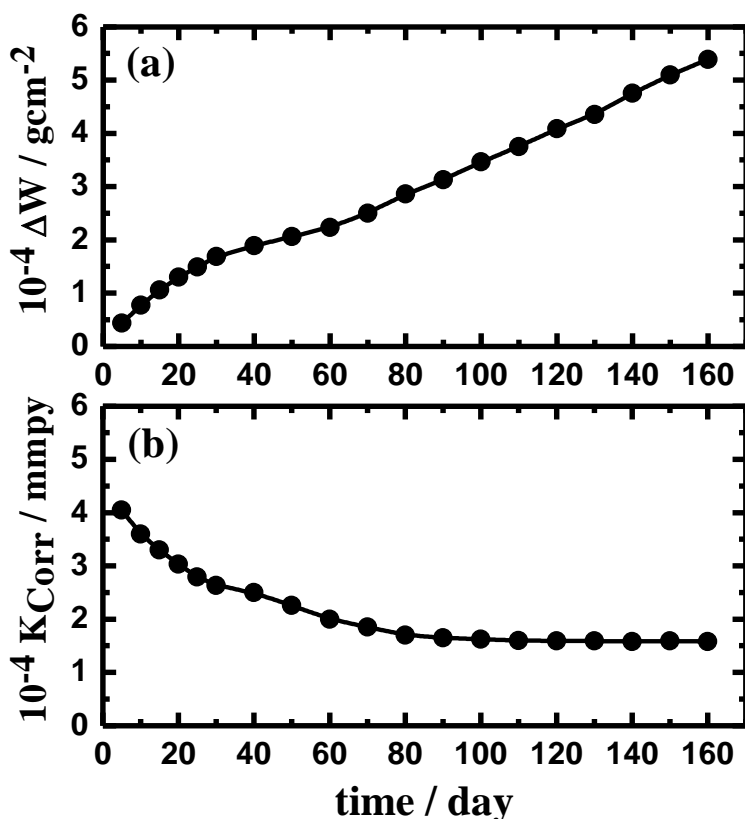


Figure 1. Variations of the weight loss (a) and corrosion rate (b) versus time for Monel-400 coupons in open to air stagnant Arabian Gulf seawater.

The atomic percentage of the elements found in the selected area of image (a) by the EDX profile, were 41.80% C, 35.28% O, 12.75% Ni, 6.33% Cu, 2.86% Cl, 0.49% Fe, 0.29% S, and 0.19% Mn. The low contents of Ni and Cu and the high percentages of C and O suggest that the alloy surface is covered with corrosion products that have different compounds, complexes and oxides. The presence of chloride, sulphur and iron besides carbon also suggest that the surface is having scales deposited from the seawater.

In order to understand the mechanism of pitting corrosion of Monel-400 in the AGS at this condition, the SEM/EDX investigations were obtained for the corrosion products around the pits as well as inside the pits. Fig. 3 depicts, (a) SEM micrograph represents a pit on the Monel-400 surface after its immersion in freely aerated stagnant AGS solution for 160 days and (b) the corresponding EDX profile analysis taken for the corrosion products around the pit as selected on the SEM image, respectively. The atomic percentage of the elements found around the pit shown in the SEM image (a), were 46.31% O, 20.76% C, 5.01% Ni, 19.12% Cu, 8.26% Cl, and 0.55% S with no Fe and Mn. The high level of O and C provide that the surface of Monel-400 around the pit is covered with a thick oxide layer with other corrosion products. The very low content of Ni compared to Cu is due to the

selective dissolution of Ni, while Cu tends to form oxide and chloride. The presence of C and S indicate that the area around pits has scale and corrosion products resulted from the components of the seawater.

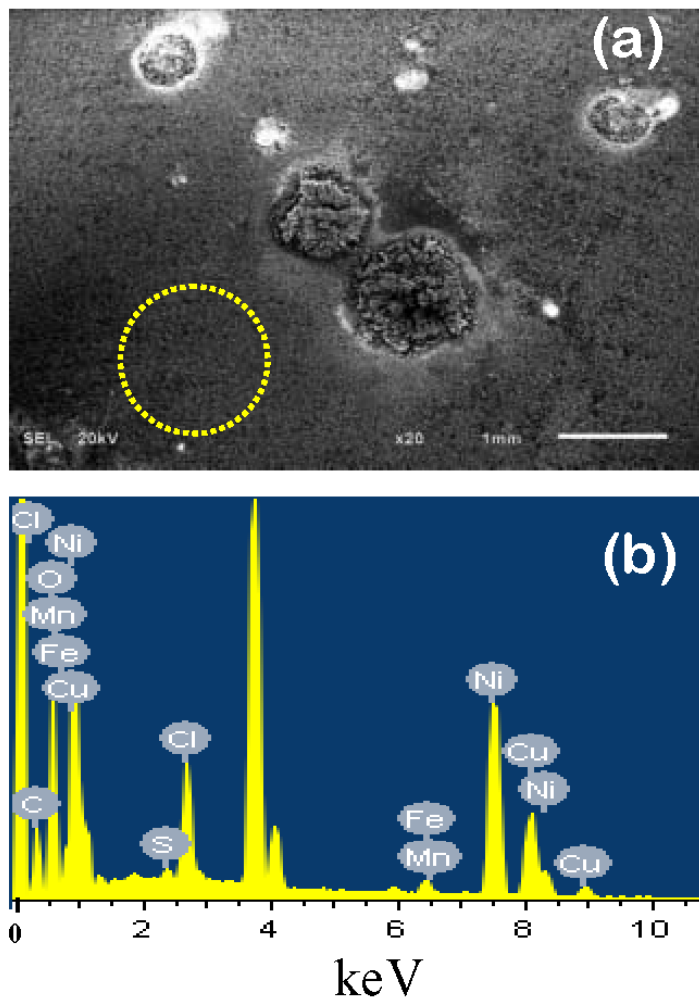


Figure 2. (a) SEM micrograph for a large area of Monel-400 surface after its immersion in freely aerated stagnant AGS solution for 160 days and (b) the corresponding EDX profile analysis taken in the selected area of the SEM image, respectively.

Figure 4 shows (a) SEM micrograph represents an extended area inside a pit was formed on the surface of Monel-400 that has been immersed in freely aerated stagnant AGS solution for 160 days and (b) the corresponding EDX profile analysis taken inside the pit as selected on the SEM image, respectively. The SEM image shows that the formed pit is deep and wide with corrosion products deposited in some areas inside it. The atomic percentages of the components found inside the pit were found to be 58.92% Cu, 17.01% Ni, 15.73% O, 6.96% Cl, 0.95% Fe, and 0.43% S. The very high content of copper (almost double of its natural presence in the alloy) as well as the very low Ni content inside the pit confirms the selective dissolution of Ni with copper enrichment. The poor presence of oxygen inside the pit compared to its percentages on the surface (35.28%) and around the pit (46.31%)

also specifies that the aggressive ions such as Cl^- displace the oxygen at its weakest bond with metal on the alloy surface and initiate pitting corrosion.

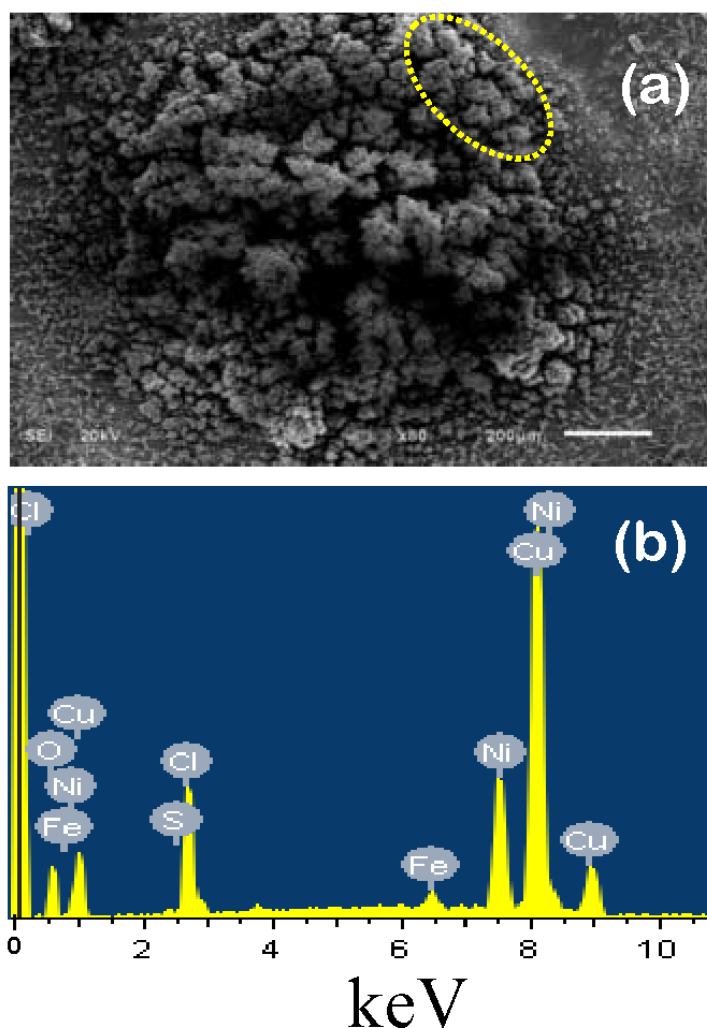


Figure 3. (a) SEM micrograph represents a pit on the Monel-400 surface after its immersion in freely aerated stagnant AGS solution for 160 days and (b) the corresponding EDX profile analysis taken for the corrosion products around the pit as selected on the SEM image, respectively.

The presence of Cl^- increases the potential difference across the passive film, thereby enhancing the rate of nickel ions diffusion from the nickel-film interface to the film-solution interface, forming cation vacancies at the Monel-film interface [5]. When the concentration of Cl^- is high enough, voids develop at the nickel-film interface. Continued growth of such voids results in the localized collapse of the passive film, which will dissolve faster than other regions of the passive film, leading to pit growth and ultimately substrate alloy dissolution [17]. It is worth to mention that the maximum pit depth measured in stagnant natural seawater for Monel-400 was 1.067 mm deep as reported in a three-year study at the Inco Test Facility [15]. The attacked regions were copper-rich while the regions around the active sites had higher Ni concentrations. This agrees with our work and

also the work reported by Gouda et al. [18] and Little et al. [19] that the corrosion of Monel-400 undergoes through the selective leaching of nickel from the alloy leaving a spongy copper –rich material in the base of the pit.

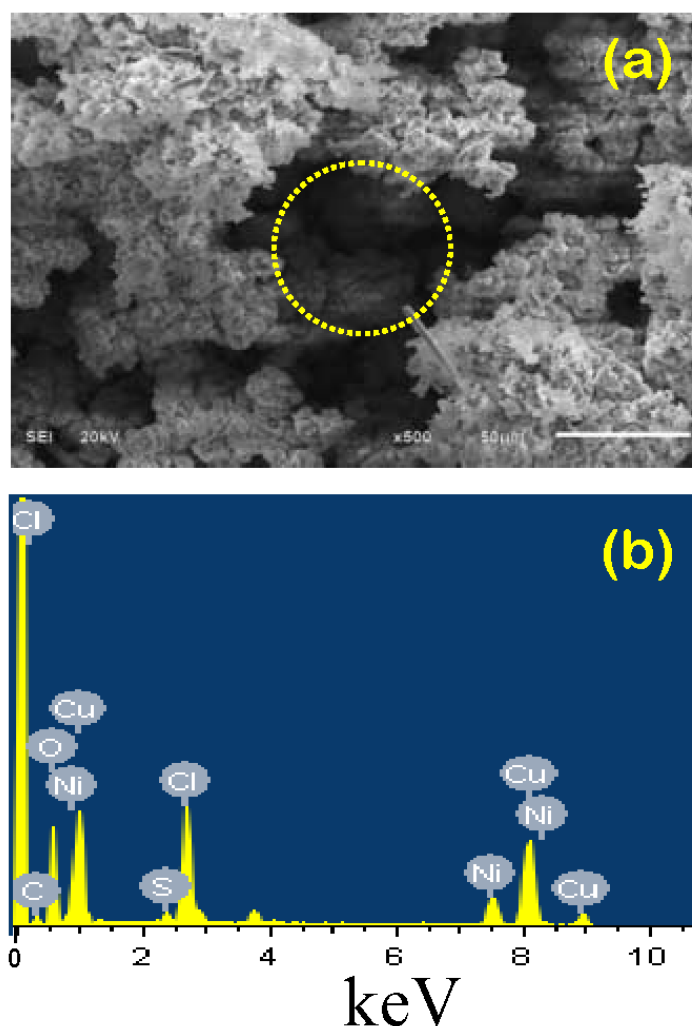


Figure 4. (a) SEM micrograph represents an extended area for a pit on the Monel-400 surface after its immersion in freely aerated stagnant AGS solution for 160 days and (b) the corresponding EDX profile analysis taken inside the pit as selected on the SEM image, respectively.

According to Little et al. [19] chlorine and sulphur from seawater accumulate within the pit and react with the iron and nickel in the alloy, which is why the percentage of Fe and Ni are lower inside the pit compared to their natural presence in the alloy.

3.2. Cyclic potentiodynamic polarization (CPP) measurements

CPP experiments were carried out after Monel immersion in AGS solutions for 0 h, 24 h, and 72 h in order to understand the mechanism of Monel dissolution after varied exposure periods. This

technique was also used to report the effect of time on the change of corrosion potential (E_{Corr}), Corrosion current (j_{Corr}), pitting potential (E_{Pit}), pitting current (j_{Pit}), polarization resistance (R_P), and corrosion rate (K_{Corr}) of Monel-400 in the test medium.

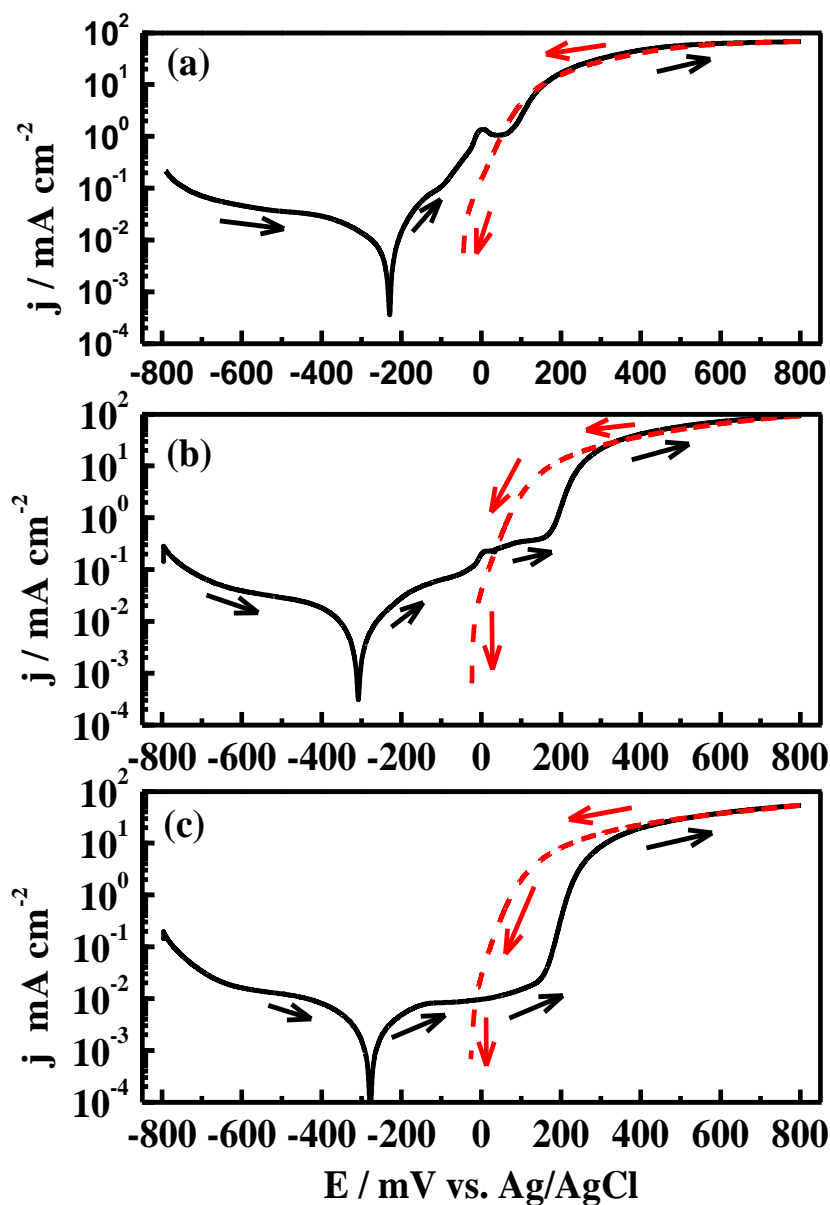


Figure 5. Cyclic potentiodynamic polarization curves for Monel-400 after 0 h (a), 24 h (b), and 72 h (c) immersion in Arabian Gulf seawater, respectively.

The CPP curves for the Monel electrode after (a) 0 h, (b) 24 h, and (c) 72 h immersion in AGS solutions, respectively are shown in Fig. 5. Blundy and Pryor [9] have reported that the anodic reaction of Monel-400 is the selective dissolution of nickel, particularly at high potential values. Gouda et al. [18] with Arabian seawater and Little et al. [19] with Gulf of Mexico water have also demonstrated

that the anodic dissolution of Monel-400 occurs due to the intergranular corrosion and selective dealloying of iron and nickel, especially in the presence of sulfate-reducing bacteria.

It is clearly seen from Fig. 5a that an active dissolution of the alloy occurred with increasing potential in the anodic side. It is also seen that there is a peak on the anodic branch at which the current decreased with increasing the applied potential. This peak was appeared due to either the formation of a passive oxide film [20, 21] or the accumulation of corrosion products on the electrode surface. The sudden increase of the current after the formation of the peak is due to the breakdown of the passive film formed on the Monel-400 surface by the attack of aggressive ions presented in the seawater such as chlorides and lead to the occurrence of pitting corrosion [22]. The further increase of the current with potential is caused by the agglomeration of chloride ions inside the pits leading to pit growth and ultimately substrate alloy dissolution [5].

Table 1. Corrosion parameters obtained from CPP curves shown in Fig. 6 for the Monel-400 in aerated stagnant Arabian Gulf seawater after different exposure intervals.

Parameter Medium	$E_{Corr}/$ mV	$j_{Corr}/$ $\mu\text{A cm}^{-2}$	$\beta_c/$ mV dec^{-1}	$\beta_a/$ mV dec^{-1}	$E_{Prot}/$ mV	$j_{Prot}/$ μAcm^{-2}	$E_{Pit}/$ mV	$j_{Pit}/$ μAcm^{-2}	$R_p/$ Ωcm^2	$K_{Corr}/$ mmy^{-1}
AGS (0h)	-250	14	120	105	51	1200	70	1050	1744	0.160
AGS (24h)	-283	5.6	125	115	36	220	160	450	4653	0.064
AGS (72h)	-278	2.9	130	125	-24	9.5	160	25	9549	0.033

Increasing the immersion time of the electrode in the AGS solution to 24 h before measurements (Fig. 5b) decreased both the anodic and peak currents and even eliminated the peak when the immersion time was increased to 72h as shown in Fig. 5b and 5c, respectively. The corrosion parameters obtained from Fig. 5 are shown in Table 1. It is seen from Table 1 that the values of j_{Corr} , j_{Prot} and j_{Pit} decreased with increasing the immersion time. Also, the values of E_{Corr} , E_{Prot} , and E_{pit} increased to the more negative values. This effect also increased the values of polarization resistance (R_p) and decreased the values of corrosion rate (K_{Corr}), which were calculated as previously reported [13, 23-25].

3.3. Chronoamperometric measurements

The variation currents versus time for Monel-400 electrode that has been immersed in the AGS solutions for (1) 0 h, (2) 24 h, and (3) 72 h, respectively before stepping the potential to 100 mV for 120 min are shown in Fig. 6. The highest current values for Monel-400 in AGS solutions were recorded when the measurements were carried out after the first moment of the electrode immersion, curve 1. It is clearly observed that the current increased with time till the end of the run. Increasing the immersion time to 24 h, (curve 2) led to decreasing the absolute current and further current decreases were recorded when the time was increased to 72 h (curve 3). This decrease in the absolute current with increasing immersion time of Monel before applying the constant potential can be explained by

the formation of a passive oxide film and/or corrosion products; this film gets even thicker as the time increases. The formation of such species on the surface decreases the uniform attack of the Monel-400 and so decreases the absolute current under the applied potential.

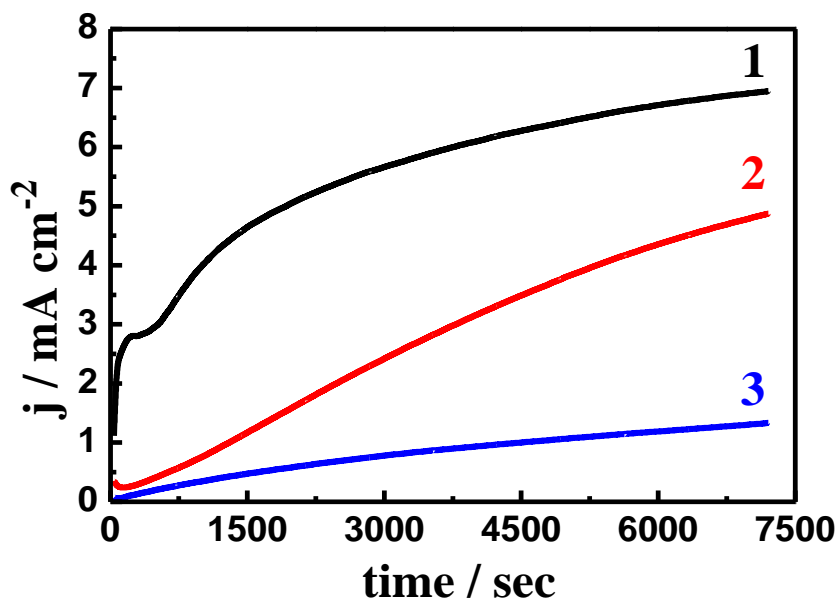


Figure 6. Chronoamperometric curves for the Monel-400 electrode that has been immersed in Arabian Gulf seawater for 0 h (1), 24 h (2) and 72 h (c) before stepping the potential to 100 mV vs. Ag/AgCl before measurements.

On the other hand, the increase of current values with time when the potential was stepped to 100 mV is due to the dissolution of the film formed on the Monel-400 surface, due to the preimmersion of the electrode in the solution, leading to the occurrence of the pitting corrosion. The higher the absolute currents the higher the number of small and narrow pits. This means that increasing the exposure time before measurement leads to decrease the number of pits at the same time it increases the width and depth of the pits formed. Pits develop [5, 26] at sites where oxygen adsorbed on the alloy surface is displaced by an aggressive species such as Cl^- ions that are presented in the AGS solution. This is because Cl^- ions have small diameters allows it to penetrate through the protective oxide film and displace oxygen at the sites where metal-oxygen bond is the weakest [5, 17].

3.4. Open-circuit potential (OCP) and electrochemical impedance spectroscopy (EIS) measurements

The variation of the OCP versus time (72 h) for Monel-400 electrode in AGS is shown in Fig. 7. It is clearly seen that the potential values slightly increased toward the more negative direction in the first 10 h due to the dissolution of Monel-400 by the aggressive ions attack that present in the AGS on the electrode surface. This slight negative potential shift decreased with increasing the immersion time

up to the first 45 h, which might be due to the formation of corrosion products including oxides on the surface.

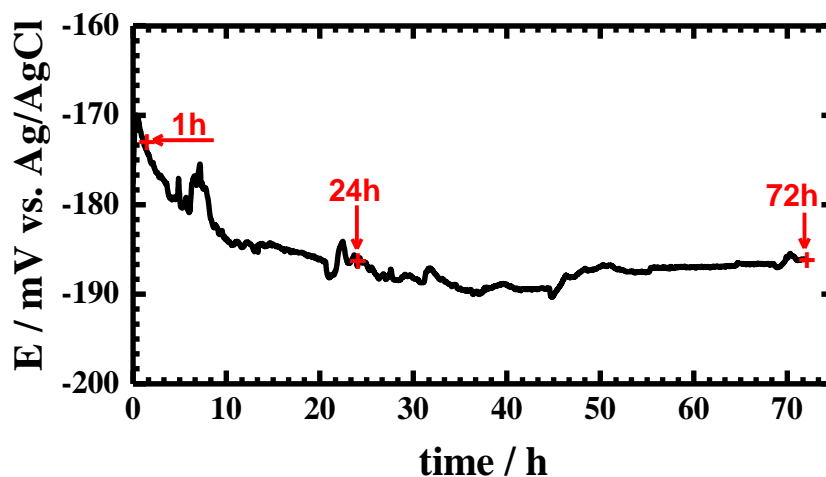


Figure 7. The change of the open-circuit potential versus time for Monel-400 in Arabian Gulf seawater.

The formation of such corrosion products partially protected the alloy surface, which is why the potential decreased in the positive direction again and till the end of the test. This very slight positive shift in the OCP values decreased the corrosion rate by decreasing the uniform attack of the alloy with time. This decrease in corrosion rate might result not only from the formation of corrosion products but also because of the ability of AGS solution to form scales on the Monel-400 surface.

The EIS measurements were carried out to determine kinetic parameters for electron transfer reactions at the Monel-400/electrolyte interface and to confirm the data obtained by CPP and CA measurements. Typical Nyquist plots (a), Bode (b), and phase angle (c) for Monel-400 after its immersion for (1) 1 h; (2) 24 h; and (3) 72 h, respectively in AGS are shown in Fig 8. It is clear from Fig. 8a that only single semicircles are observed for the Monel electrode in AGS for the different exposure intervals. The chord length pertaining to the high frequency (HF) loop observed in Nyquist diagram increased as the immersion time before measurements increased. This increase of the HF chord is due to the decrease in the electrochemical active areas by the accumulation of corrosion products and oxides at the Monel surface. The diameter of the semicircle is significantly increased with increasing the time of exposure to 24 h and further to 72 h. It has been reported that the semicircles at high frequencies are generally associated with the relaxation of the capacitors of electrical double layers with their diameters representing the charge transfer resistances [24, 27].

The Nyquist spectra shown in Fig. 8a were analysed by fitting to the equivalent circuit model shown in Fig. 9 and was also used previously to fit the impedance data obtained for Monel-400 in simulated seawater [28]. The parameters obtained by fitting the equivalent circuit shown in Fig. 9 are listed in Table 2.

Table 2. EIS parameters obtained by fitting the Nyquist plots shown in Fig. 8a with the equivalent circuit shown in Fig. 9 for the Monel-400 in aerated stagnant Arabian Gulf seawater after different exposure intervals.

Parameter Medium	$R_s / \Omega\text{cm}^2$	Q (CPEs)		$R_{P1} / \Omega\text{cm}^2$	$C_{dl} / \mu\text{Fcm}^{-2}$	$R_{P2} / \Omega\text{cm}^2$
		$Y_Q / \mu\text{Fcm}^{-2}$	n			
AGS (1h)	3.35	44.32	0.46	2810	3.881	5610
AGS (24h)	6.46	33.94	0.48	4030	0.445	9722
AGS (72h)	7.45	16.77	0.58	8210	0.335	13400

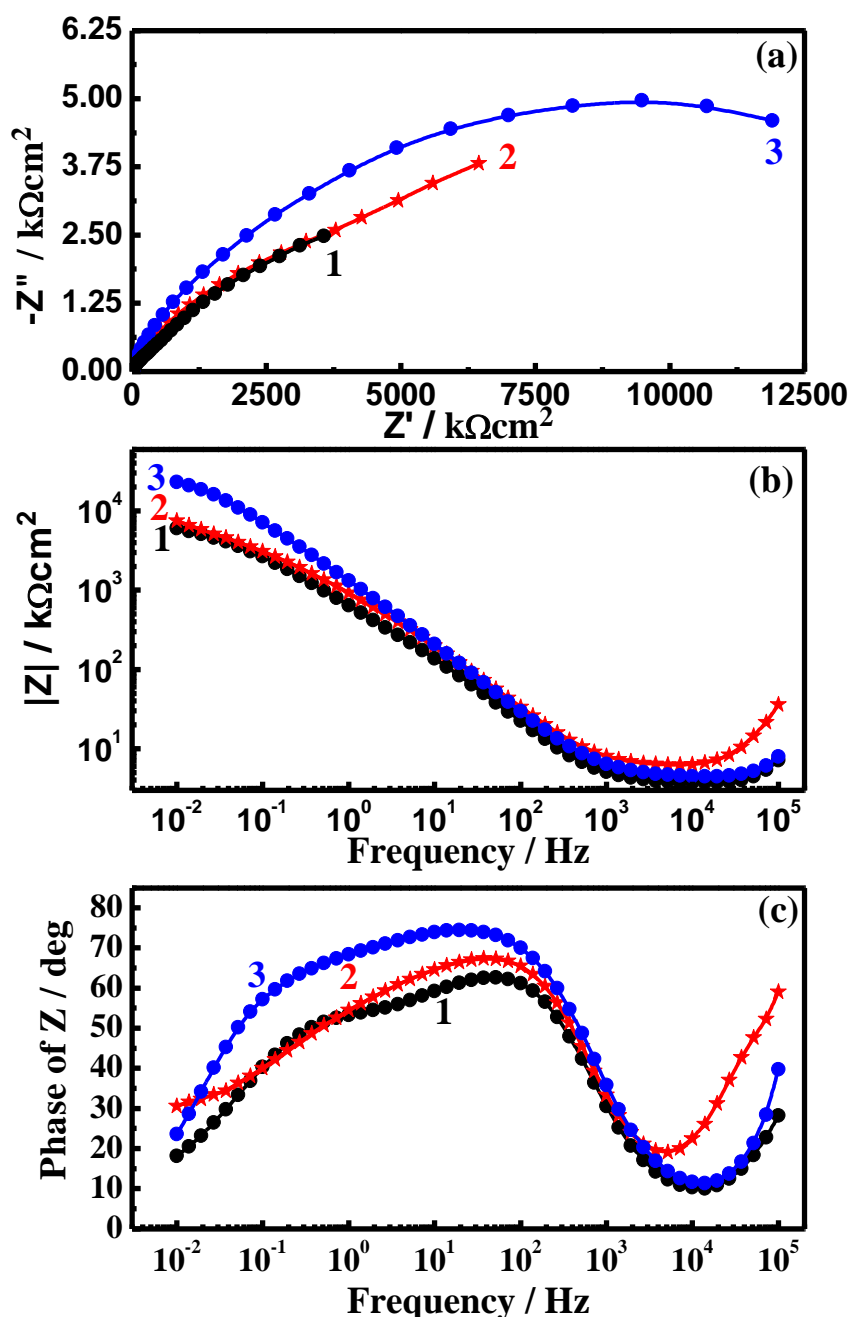


Figure 8. Nyquist (a), Bode (b) and phase angle (c) plots for Monel-400 at OCP ($E_{\text{Corr}} \pm 5$ mV) after its immersion in Arabian Gulf seawater for 1 h (1), 24 h (2), and 72 h (3).

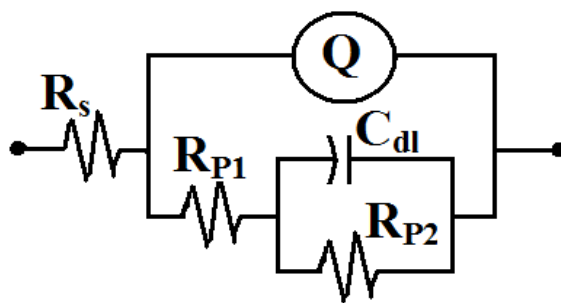


Figure 9. The equivalent circuit used to fit the experimental data presented in Fig. 8a.

According to usual convention, R_s represents the solution resistance between the Monel surface and the platinum counter electrode, Q the constant phase elements (CPE) and contain two parameters; a pseudo capacitance and an exponent (an exponent close to 0.5), the R_{P1} accounts for the resistance of a film layer formed on the Monel-400 surface, C_{dl} is the double layer capacitance, and R_{P2} accounts for the charge transfer resistance at the alloy surface, i.e. the polarization resistance. It is seen from Fig. 8 and Table 2 that the values of R_s , R_{P1} and R_{P2} increased as the immersion time of Monel in AGS before measurements was increased. The polarization resistance measured by EIS in this case is a measure of the uniform corrosion rate as opposed to tendency towards localized corrosion. The increase of the resistances ($R_P = R_{P1} + R_{P2}$) in this case is attributed to the formation of a passive film and/or corrosion products, which gets thicker with time and could lead to the decrease in j_{CORR} and K_{CORR} and also the increase in R_P values we have seen in CPP experiments, Fig. 5 and Table 1, under the same conditions. The CPE, Q , is almost like Warburg impedance with its n -values smaller than 0.50, suggesting that the formed corrosion products and oxide layer on the Monel-400 surface block the mass transport acting like a resistor. The values of Y_Q decreased with time indicating that the dissolution of Monel is also limited by mass transport. That was again confirmed by the decrease of the double layer capacitance, C_{dl} , values with increasing the immersion time.

The results presented by Nyquist plots and Table 2 were also supported by the increase in the impedance of the interface with increasing the exposure interval of Monel before measurement as shown in Fig. 8b. It has been reported [29–37] that the increase of the impedance and low frequency values means the increase of the passivation of the surface. Further confirmation is also provided by the increase of the maximum phase angle (Fig. 8c) with time at the same conditions. In general, the EIS data is in good agreement with the electrochemical (CPP and CA) experiments and weight loss measurements.

4. CONCLUSIONS

The corrosion of Monel-400 alloy in stagnant Arabian Gulf seawater (AGS) has been studied by using gravimetric and electrochemical measurements in addition to SEM/EDX investigations. The loss in weight data indicated that Monel-400 suffers both general and localized corrosion. Pitting

corrosion occurred for Monel due to the attack of corrosive species such as Cl^- to the weakest oxygen-Alloy bond and that a selective dissolution of Ni leads to the propagation of the formed pits as shown by SEM/EDX investigations. Cyclic polarization, OCP and EIS measurements revealed that the increase of exposure time decreases the corrosion current and increases the polarization resistance as well as shifts pitting and protection potentials to the more negative direction. Chronoamperometric curves proved that the severity of pitting corrosion increases and the uniform attack decreases for Monel with increasing immersion time. In general, the electrochemical measurements confirmed the data obtained by gravimetric ones that the uniform attack decreases, while pitting corrosion increases with increasing the exposure time of Monel in the AGS solution.

ACKNOWLEDGEMENT

The authors are grateful to the Center of Excellence for Research in Engineering Materials (CEREM) for the financial support.

References

1. J.A. Ali, J.R. Ambrose, *Corros. Sci.*, 32 (1991) 799.
2. C.J. Semino, P. Pedferri, G.T. Burstein, T.P. Hoar, *Corros. Sci.*, 19 (1979) 1069.
3. S.K. Ghosh, G.K. Dey, R.O. Dusane, A.K. Grover, *J. Alloy. Compd.*, 426 (2006) 235.
4. S. Hettiarachchi, T.P. Hoar, *Corros. Sci.*, 19 (1979) 1059.
5. V.K. Gouda, I.Z. Selim, A.A. Khedr, A.M. Fathi, *J. Mater. Sci. Technol.*, 15 (1999) 208.
6. J.A. Ali, *Corros. Sci.*, 36 (1994) 773.
7. H.P. Lee, Ken Nobe, *J. Electrochem. Soc.*, 131 (1984) 1236.
8. M.E. Walton, P.A. Brook, *Corros. Sci.*, 17 (1977) 317.
9. R.G. Blundy, M.J. Proyor, *Corros. Sci.*, 12 (1972) 65.
10. M. Metikoš-Huković, R. Babić, I. Škugor, Z. Grubač, *Corros. Sci.*, 53 (2011) 347.
11. Saleh A. Al-Fozan, Anees U. Malik, *Desalination*, 228 (2008) 61.
12. A.M. Shams El Din, M.E. El Dahshan, A.M. Taj El Din, *Desalination*, 130 (2000) 89.
13. E.M. Sherif, S.-M. Park, *Corros. Sci.*, 48 (2006) 4065.
14. J. Tang, Yawei Shao, Tao Zhang, Guozhe Meng, Fuhui Wang, *Corros. Sci.*, 53 (2011) 1715.
15. J.R. Davis, ed., *Metals Handbook*, 2nd Ed. Materials Park, OH: ASM International, 1998.
16. V.K. Gouda, H.M. Shalaby, *Corros. Sci.*, 35 (1993) 683.
17. J.A. Ali, J.R. Ambrose, *Corros. Sci.*, 33 (1992) 1147.
18. V.K. Gouda, I.M. Banat, W.T. Riad, S. Mansour, *Corrosion*, 49 (1993) 63.
19. B. Little, P. Wagner, R. Ray, J.M. Jones, *Corrosion*, Paper No. 101(1991).
20. W.Z. Friend, ed., "Corrosion of Nickel and Nickel-Based Alloys", Houston, TX: NACE International (1980).
21. M. Stern, *J. Electrochem. Soc.*, 106 (1959) 376.
22. M.A. Streicher, *J. Electrochem. Soc.*, 103 (1956) 375.
23. E.-S.M. Sherif, A. A. Almajid, *Int. J. Electrochem. Sci.*, 6 (2011) 2131.
24. E.-S.M. Sherif, *Int. J. Electrochem. Sci.*, 6 (2011) 1479.
25. E.-S.M. Sherif, R. M. Erasmus, J. D. Comins, *Electrochim. Acta*, 55 (2010) 3657.
26. H. Bohni, *J. Electrochem. Soc.*, 116 (1969) 906.
27. H. Ma, S. Chen, L. Niu, S. Zhao, S. Li, D. Li, *J. Appl. Electrochem.*, 32 (2002) 65.
28. R.D. Klassen, P.R. Roberge, Y. Wang, *Corrosion*, Paper No. 05232, NACE International, Houston, Texas (2005).

29. E.-S.M. Sherif, *Int. J. Electrochem. Sci.*, 6 (2011) 3077.
30. E.-S.M. Sherif, *Mater. Chem. Phys.*, 129 (2011) 961.
31. E.-S.M. Sherif, *J. Mater. Eng. Perform.*, 19 (2010) 873.
32. E.-S.M. Sherif, A.A. Almajid, *J. Appl. Electrochem.*, 40 (2010) 1555.
33. E.-S.M. Sherif, A.A. Almajid, F.H. Latif, H. Junaedi, *Int. J. Electrochem. Sci.*, 6 (2011) 1085.
34. E.-S.M. Sherif, *Int. J. Electrochem. Sci.*, 6 (2011) 2284.
35. E.-S.M. Sherif, A.H. Ahmed, *Synthesis and Reactivity in Inorganic, Metal-Organic and Nano-Metal Chemistry*, 40 (2010) 365.
36. E.-S.M. Sherif, J.H. Potgieter, J.D. Comins, L. Cornish, P.A. Olubambi, C.N. Machio, *J. Appl. Electrochem.*, 39 (2009) 83.
37. E.-S.M. Sherif, J.H. Potgieter, J.D. Comins, L. Cornish, P.A. Olubambi, C.N. Machio, *Corros. Sci.*, 51 (2009) 1364.